Extruded colour-based plastic film for the measurement of dissolved CO_2

Andrew Mills* and Dilidaer Yusufu

Queens University Belfast, David Keir Building, Stranmillis Road, Belfast, BT9 5AG, UK

Email: andrew.mills@qub.ac.uk

Abstract

Dissolved CO_2 measurements are usually made using a Severinghaus electrode, which is bulky and can suffer from electrical interference. In contrast, optical sensors for gaseous CO_2, whilst not suffering these problems, are mainly used for making **gaseous** (not dissolved) CO_2 measurements, due to dye leaching and protonation, especially at high ionic strengths (> 0.01M) and acidity (< pH 4). This is usually prevented by coating the sensor with a gas-permeable, but ion-impermeable, membrane (GPM). Herein, we introduce a highly sensitive, colourimetric-based, plastic film sensor for the measurement of both **gaseous** and **dissolved** CO_2, in which a pH-sensitive dye, thymol blue (TB) is coated onto particles of hydrophilic silica to create a CO_2-sensitive, TB-based pigment, which is then **extruded** into low density polyethylene (LDPE) to create a GPM-free, i.e. naked, TB plastic sensor film for gaseous and dissolved CO_2 measurements. When used for making dissolved CO_2 measurements, the hydrophobic nature of the LDPE renders the film: (i) indifferent to ionic strength, (ii) highly resistant to acid attack and (iii) stable when stored under ambient (dark) conditions for > 8 months, with no loss of colour or function. Here, the performance of the TB plastic film is primarily assessed as a **dissolved** CO_2 sensor in highly saline (3.5 wt%) water. The TB film is blue in the absence of CO_2 and yellow in its presence, exhibiting 50% transition in its colour at ca. 0.18% CO_2. This new type of CO_2 sensor has great potential in the monitoring of CO_2 levels in the hydrosphere, as well as elsewhere, e.g. food packaging and possibly patient monitoring.

Key words: thymol blue, LDPE, extrusion, carbon dioxide, optical sensor, salt water

1. Introduction

Carbon dioxide (CO_2) is a key parameter in many biological and biochemical process [1-3] and so it follows that the measurement of CO_2 is important in many different fields [4-7], not least of which is the monitoring of dissolved CO_2 in the hydrosphere, i.e. oceans, river, lakes and streams [1, 8-10].

Many different methods have been used to measure CO_2 in air and in water, including: gas chromatography [11], titrimetry [12], coulometry [13], amperometry [14], potentiometry (including ISEs and ISFETS) [6,15,16], UV/Vis spectrophotometry [17,18] and IR spectrometry [19]. Obviously, any methods that require reagents, regular sample taking and/or pumps are inappropriate for long-term, *in-sit*u deployment, and under such circumstances solid state sensors, such as optodes [20] and potentiometric devices [6,15,16,21,22] appear more appropriate.

The most commonly used sensor for dissolved CO_2 measurements is the Severinghaus electrode [6, 15], which comprises a pH electrode in contact with a thin layer of bicarbonate buffer solution, with the whole system encapsulated by a thin, gas-permeable, but ion-impermeable membrane (referred to henceforth as a 'GPM'), such as PTFE. In a Severinghaus electrode, a change in the ambient level of dissolved CO_2 produces a change in the pH of the bicarbonate layer, which is detected by the encapsulated pH electrode. However, the Severinghaus electrode is usually quite bulky and susceptible to electrical interference.

There has been increasing interest over the last 24 years in solid-state, CO_2-sensitive optical sensors [23-25]. Such sensors, like the Severinghaus electrode, are usually based on the acidic nature of dissolved CO_2, and use an embedded fluorescent, or colourimetric, pH sensor to detect the CO_2-induced pH change in the sensor layer. The most popular of these solid-state optical sensors employs a quaternary ammonium hydroxide salt, $Q^+OH^-.xH_2O$, (a phase transfer agent) to create a solvent-soluble version of the deprotonated form of the pH indicating dye, D^-, i.e. $Q^+D^-.xH_2O$, which can then be incorporated in a solvent-based ink, containing a lipophilic polymer, which, in turn, can be cast onto an inert substrate, such as glass or Mylar®, to yield a CO_2-sensitive optical film.

The general mechanism of the above phase transfer optical CO_2 sensor [23-25], referred to henceforth as a 'PT CO_2 sensor', is summarised by the following reaction equation,

$$Q^+D^- . xH_2O + CO_2 \rightleftharpoons Q^+HCO_3^- . (x-1)H_2O + DH \quad (1)$$

Colour/Fluorescence A Colour/Fluorescence B

in which the deprotonated pH sensitive dye, $Q^+D^-.xH_2O$, is reversibly protonated, when CO_2 is present, to form $Q^+HCO_3^-.(x\text{-}1)H_2O.DH$, resulting in a colour (or fluorescence) change, from A to B, which is similar to that seen in aqueous solution when the free dye, D^-, is protonated by an acid to form DH. The PT CO_2 sensor relies on the water of hydration of the ion-pair to interact with the CO_2 to form reversibly the lipophilic species: $Q^+HCO_3^-.(x\text{-}1)H_2O$ and, simultaneously, the differently coloured/fluorescent species, DH. The CO_2-sensitivity of the PT CO_2 sensor can be adjusted by varying the base concentration and by using pH indicating dyes with different pK_a's. Not surprisingly, given reaction (1), this type of sensor responds equally well to dry and humid CO_2-containing gases.

The attractions of using such optical sensors for CO_2, rather than the Severinghaus electrode for example, include: (1) freedom from electrical interference, (2) easily miniaturised, (3) ideal for remote sensing, (4) rapid in response, (5) inexpensive and simple to make and, (6) usually disposable [25]. A major weakness of the PT CO_2-optical sensor is a low stability when placed in direct contact with water, since this often leads to: (i) leaching of the pH-sensor dye, particularly in high ionic strength, i.e. salty, water and (ii) proton interference, especially under acidic conditions (i.e. usually pH < 4). As a result, although there have been many reports of PT **gaseous** CO_2 sensors, there are relatively few for **dissolved** CO_2, especially in salty or acidic solution. In general, those that have been reported for such work combine a PT gaseous CO_2 sensor with a surface coating of a GPM, such as PTFE or silicone.

A list of some of the reported different solid-state, dissolved CO_2 PT optical sensors is given in table 1, along with short notes regarding their formulation, sensitivity and storage stability.

Table 1: Examples of solid-state, PT dissolved CO_2 optical sensors

Type	dye	base	Encapsulation medium/ gas permeable membrane	%CO2 (S=1/2)	storage	Ref
Colour-based	MCP	TOAH	EC/EC[a]	1.00	up to 2 days	26
	TB	borate/ bicarbonate	HS water/silicone	0.01	>4 days	27
	BTB	TOAH	ionic liquids (RTILs)/none	60.00	1 month	28
Fluorescence-based	HPTS	TOAH	EC/Teflon	0.30	several days	29
	HPTS	TOAH	silicone/silicone	10.00	over 5 months	30
	HPTS	TOAH	EC/EC	0.6[b,c]	<5 days	31, 32

MCP: meta-cresol purple; TB: thymol blue; BTB: bromothymol blue; HPTS: 8-hydroxypyrene-1,3,6-trisulfonate; TOAH: tetraoctylammonium hydroxide; EC: ethyl cellulose; HS water: highly saline water; [a]:only stable when pH≥6 and ionic strength ≤ 0.01M; [b]: based on dual-lifetime referencing (DLR); [c]: characterised in gaseous CO_2.

From the entries in table 1 it is clear that most reported solid state PT dissolved CO_2 sensors utilise a GPM in order to prevent dye leaching and/or protonation by the solution under test. Interestingly, an exception appears to be the fluorescent-based, PT dissolved CO_2 sensor sold currently by PreSens GmbH [31,32], which appears to be sold in a naked, i.e. GPM free, form. However, and perhaps not surprisingly, the manufacturer reports that the latter displays 'cross-sensitivity to ionic strength (salinity)' and cannot be used at 'pH above 10 or below 4'. It is worth noting here too that a quite different optical sensor for CO_2 has been reported recently, which uses a highly selective carbonate ionophore, coupled to a highly basic pH sensor, encapsulated in a polymeric film [20]. The latter responds well to CO_2 in both air and dissolved in water, but suffers chloride interference when used in sea water and cannot be used much below pH 4.8 [20,22]. Consistent with most work on other CO_2 optical sensors, the authors suggest that these problems may be avoided by adding a GPM layer to the optical sensor [20].

As indicated by the data in table 1, another common drawback exhibited by many PT CO_2 sensors is an inherent short shelf-life, probably due to the presence of other acidic gases, such as SO_2 or NO_2 in the atmosphere, that irreversibly protonate the sensor film [31]. Other, more recent, work shows that ambient humidity and sensor film water content are also important factors in determining PT CO_2 sensor shelf-life, and that usually the higher the relative humidity the greater the shelf-life [30]. These shelf life issues, and the apparent need for special storage conditions, represent a barrier to the large-scale commercialisation of the PT CO_2 sensor technology.

In a recent paper, this group reported on a naked, i.e. no GPM layer, low density polyethylene (LDPE) plastic fluorescence-based PT CO_2 sensor [33], created by blending, in an extruder, the LDPE with a CO_2-sensitive pigment, comprising a coating of the fluorescent, pH-sensitive, dye (HPTS) on hydrophilic, fumed silica. The sensor film was studied mainly as a sensor for **gaseous** CO_2, but some additional preliminary work revealed it to be very stable and functional when used directly, i.e. in its naked form, in aqueous solution to monitor **dissolved** CO_2. In addition, the HPTS-LDPE film appeared very stable when stored under ambient conditions in the dark.

Here we describe the results of a more substantial study of the optical sensing of dissolved CO_2, using an extruded, **naked**, plastic, **colour**-based, solid-state PT CO_2 sensor, since, unlike fluorescence, absorbance changes can be readily detected by eye and monitored inexpensively using digital camera technology, coupled with RGB analysis [34]. The study is focussed largely on the measurement of **dissolved** CO_2 in highly saline water, i.e. under conditions that are usually considered operationally highly challenging, if not impossible, for **all** naked CO_2 optical sensors.

2. Experimental

2.1. Materials

In this work, Thymol Blue (TB) was chosen as the colour-based CO_2 sensor dye, as it has found widespread use in this role, due to its moderate pK_a (= 8.9), striking colour change (blue in its deprotonated form, TB^-, and yellow in its protonated form, HTB) and low cost.

The thymol blue sodium salt (TB) was purchased from Sigma Aldrich (95%, 861367-5G), and used as received, as was the water-soluble base, tetrabutyl ammonium hydroxide, TBAH, 40 wt% in water, i.e. $Q^+OH^-.xH_2O$, where Q^+ = tetrabutyl ammonium cation. The latter was used to create the ion-pair, $Q^+D^-.xH_2O$, in reaction (1), where D^- is TB^-, which was then coated onto particles of hydrophilic fumed silica, Aerosil 130, a gift from Evonik (BET surface area = 130 ± 25 $m^2\ g^{-1}$), so as to create the PT-based, CO_2 -sensitive TB-pigment, *vide infra*.

The low-density polyethylene, LDPE, used to make the plastic films, was supplied by PW Hall UK in powder form, melt flow index, MFI, 20, for masterbatch manufacture, and the LDPE pellets (MFI = 4), for final film production, were provided by Ultrapolymers UK. All gases used were high purity and included pure CO_2 and Ar. Individual mixtures of: (i) 5% CO_2/air, (ii) 1% CO_2/air mixture and (iii) 0.1% CO_2/air were purchased from BOC and used as received. Gas mixtures with other loadings of CO_2 were generated using a Cole Parmer gas blender, which allowed a chosen CO_2/air mixture, i.e. (i), (ii) or (iii) described above, to be blended with Ar. For CO_2 work in which the gas had a relative humidity (RH) of 100%, the CO_2-containing gas under test was sparged through two Drechsel bottles, both half-full with water, connected in series, before exposure to the CO_2 sensor. In this work, highly saline water is used, and referred to throughout as '**HS**' water, and contained 3.5 wt% NaCl (i.e. 0.60 M), which is that usually found in seawater.

2.2. TB pigment preparation

0.2 g of TB were fully dissolved in the mixture of 3 ml of a 40% TBAH aqueous solution and 100 ml of ethanol in a 250 ml round-bottomed flask. 2 g of hydrophilic silica were then added, and the mixture stirred for 2.5 h, after which the solvent was removed under reduced pressure using a rotary evaporator. The final, dry blue TB pigment powder in the round-bottomed flask was then ground into a fine powder using a mortar and pestle. The above process produces hydrophilic silica particles coated with the blue $Q^+D^-.xH_2O$, salt, where Q^+ = tetrabutyl ammonium cation and D^- is the deprotonated form of the thymol blue, TB^-, referred to throughout as the TB pigment. The indicator film coating on the silica particles is due to physical adsorption only. The TB-pigment appears blue in the absence of 100% CO_2, and yellow in its presence, as illustrated by the photographs of the two different forms of the TB pigment powder in Fig. 1.

Fig. 1. TB pigment (from left to right) in the absence and presence of 100% CO_2.

2.3. TB plastic sensor film fabrication

The CO_2-sensitive TB plastic film was fabricated via the extrusion of a mixture of the TB-pigment with low-density polyethylene (LDPE), thereby producing a final pigment loading of 5 wt%, using a Rondol Microlab 10 mm twin screw extruder (barrel L/D 25/1). Thus, 2 g TB-pigment and 18 g LDPE powder (melt flow index, MFI, 20) were mixed to produce 10 wt% pigmented powder, which was then extruded as a 2 mm diameter 'string' of a 10 wt% of TB pigmented LDPE master-batch, which was fed into an on-line pelletiser to create 3 mm long pellets. The above production method used a processing temperature that increased gradually from 90°C at the feed zone, to 140°C at the die, and a pigment/LDPE mixture feed hopper rate of 41 rpm. The extruder screw speed was 80 rpm and the pelletizer speed was 0.5 m min^{-1}.

The 3 mm long masterbatch pellets were then 'diluted' by 50% w/w using the LDPE pellets (MFI 4), to produce the final 5 wt% TB pigment in LDPE loading required for the final extruded TB–LDPE film. The thermal processing conditions for producing the TB pigmented LDPE extruded film, i.e. the 'TB– film', were: 90°C (at the feed zone), increasing to 110–125–135°C (across the barrel) and finally 140°C (at the die zone). The feed hopper rate was 20 rpm, the extruder screw speed was 80 rpm, and the extruded film take-off speed was 1.7 m min^{-1}. The final plastic film product, a 5 wt% pigmented TB plastic film (central thickness 47.5 $\pm$ 2.5 µm), was blue/green-coloured in the absence of CO_2, indicating the dye was in its deprotonated, TB^-, form, but rapidly turned yellow upon exposure to a stream of CO_2, due to the formation of HTB. Photographs of the film in these two different states are illustrated in Fig. 2.

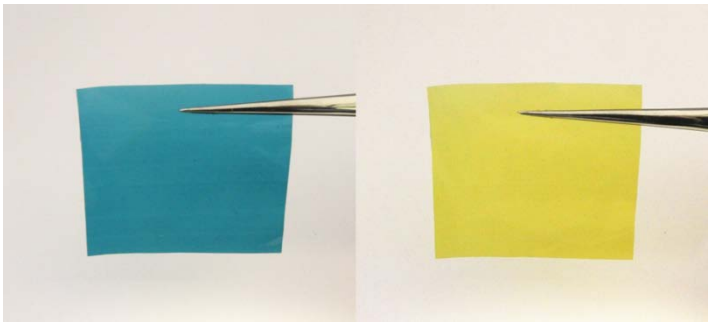

Fig. 2. Extruded TB plastic film (from left to right) in the absence (in Ar) and presence of CO_2.

The batch to batch reproducibility of the film manufacture was > 95%, as was the reproducibility within a batch, and in both cases this appears to be due mainly to small variations in film thickness; thus, if produced on a commercial scale these small variances would be reduced much further.

2.4. Measurements

All UV/ Vis absorbance measurements were made using an Agilent Technologies CARY 60 UV-vis spectrophotometer and all diffuse reflectance spectra were recorded using a KONICA MINOLTA Spectrophotometer (CM-2500d). Unless stated otherwise, all experiments were conducted at 21°C and, before any absorbance measurements were made, the spectrophotometric cell, containing the TB film, was flushed with the CO_2-containing gas under test for at least 15 min.

When used as a dissolved CO_2 sensor, the TB plastic film was always pre-soaked in the HS water for at least 24 h before use, since, during this time the background absorbance of the film increased a little (Δabsorbance, at λ = 513 nm = 0.09) due to a slight haziness, due to the uptake of water by the film. No further changes were observed in the film after this 24 h period, even when stored in HS water for weeks. When used as a dissolved CO_2 sensor, the soaked TB plastic film was placed in a spectrophotometer cell containing the HS water and the CO_2-containing gas, of known composition, was then bubbled gently (flow rate = ca. 0.2 ml s^{-1}) through the cuvette via a syringe needle for at least 45 min, to ensure full equilibration, before any absorbance measurements were made. In the study of the effect of temperature on the sensitivity of the TB sensor towards dissolved CO_2, temperature control was achieved using a thermostatted cuvette holder.

3. Results and discussion

3.1. Theory

The TB plastic film CO_2 indicator comprises a classic PT colourimetric CO_2-sensitive ink coating on hydrophilic silica particles that are embedded in a film of LDPE. A schematic of the key features of the TB plastic film is given in Fig. 3, including the identification of the main reaction species involved in the colour-changing process, as summarised by reaction (1). As noted earlier, in all the work described here, the TB plastic film used had NO additional GPM, i.e. they were always used in its, as produced, i.e. naked, form. From Fig. 3 it is clear that by embedding the indicator in the highly hydrophobic LDPE, the latter acts not only as the encapsulation material but as an intrinsic GPM, rendering redundant the need for an external GPM coating, as favoured by most optical sensors for dissolved CO_2, and so simplifying the fabrication of a PT colorimetric CO_2-sensitive sensor for such work.

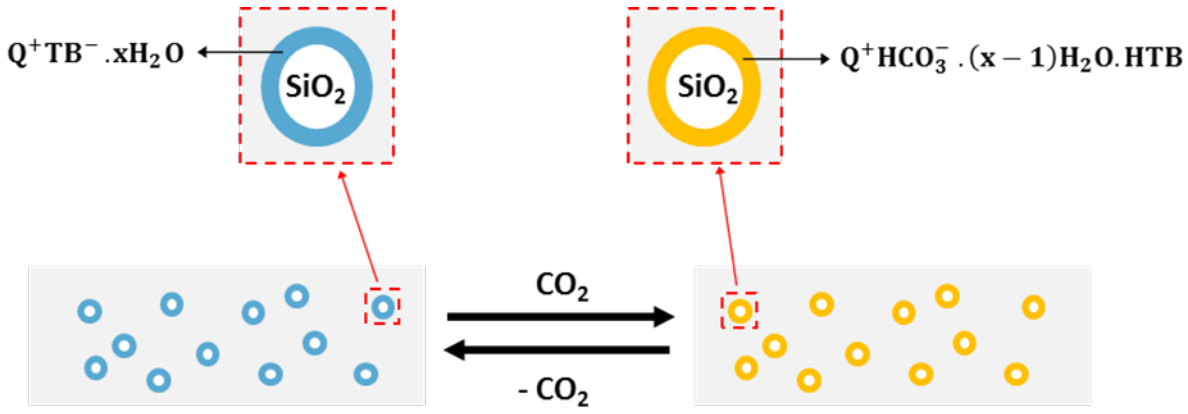

Fig. 3. Schematic of the key features and reactions of a naked, i.e. no additional GPM, extruded TB plastic film, comprising an LDPE film pigmented with hydrophilic silica particles coated with $Q^+TB^-.xH_2O$ salt, where Q^+ = tetrabutyl ammonium cation.

Given the TB-based CO_2 sensor pigment particles, embedded in the LDPE, are a classic example of a PT CO_2 indicator, with a response based on reaction (1), it is worthwhile identifying the usual terms and equations used to describe the response of such a sensor. For example, the general parameter, *R*, is the ratio of the concentrations of the protonated to deprotonated forms of the dye, and is calculated using the experimentally measured absorbance, for a colour-based CO_2 sensor at a known $\%CO_2$, made at the wavelength of maximum absorbance for D^- alone, i.e. absorbance (A) at $\lambda_{max}(D^-)$. Thus,

$$R = (A_0 - A)/ (A - A_\infty) = [HD]/[D^-] \quad (2)$$

where [HD] and $[D^-]$ are the concentrations of the protonated and deprotonated forms of the dye, respectively. A_0 is the value of absorbance due to the dye at $\lambda_{max}(D^-)$ when $\%CO_2$ = 0 (i.e. when all the dye is in its deprotonated form) and A_∞ is the absorbance of the film when all the dye is in its protonated form, HD, i.e. when $\%CO_2 = \infty$. In this work, a value for the latter was obtained by exposing the indicator to 100% CO_2. Combining equation (2) with an expression for the equilibrium constant for reaction (1), it follows that:

$$R = [HD]/ [D^-] = \alpha \times \%CO_2 \quad (3)$$

where α is a proportionality constant (units: $\%^{-1}$) which is directly related to the equilibrium constant for reaction (1) and provides a measure of the sensitivity of the CO_2 optical sensor under test [35]. Other work shows that the value of α is inversely dependent upon the background base concentration, $[Q^+OH^- .xH_2O]$ [25,26], as well as dye pK_a and temperature [24,36,37].

A more accessible, direct measure of the sensitivity of a CO_2 optical sensor is provided by the value of the $\%CO_2$ at which the normalised optical signal, S, is equal to ½ and R = 1, henceforth referred to as $\%CO_2$(S=1/2). At the $\%CO_2$(S=1/2) for an indicator film, the concentrations of the protonated and deprotonated forms of the dye are the same, R = 1 and so, from eqn (3), $\%CO_2(S=1/2) = 1/\alpha$. It is more convenient to use $\%CO_2$(S=1/2) values to compare the sensitivities of different CO_2 sensors, than refer to their calculated values of α, and, clearly, the lower the value of $\%CO_2$(S=1/2) for CO_2 sensor based on reaction (1), the greater its sensitivity.

3.2. The TB-pigment

The diffuse reflectance spectra of a sample of the TB-pigment powder under an argon (i.e. 0% CO_2) and 100% CO_2 were measured using a Minolta diffuse reflectance spectrometer. In making these measurements, 4 g of the TB-pigment were placed in a 14 ml glass vial with a plastic cap, and the gases under test, i.e. either pure Ar or CO_2, were then purged through the vial for 2 min before recording the diffuse reflectance spectra of the pigment. The results of this work are illustrated in Fig. 4 and reveal that the TB-pigment has UV/Vis

absorption peaks at 620 nm in the absence of CO_2 (due to its deprotonated, TB^-, blue/green form) and at 440 nm in the presence of CO_2 (due to its protonated HTB yellow form). The CO_2-induced colour changes were very fast (< 1 s) and reversible.

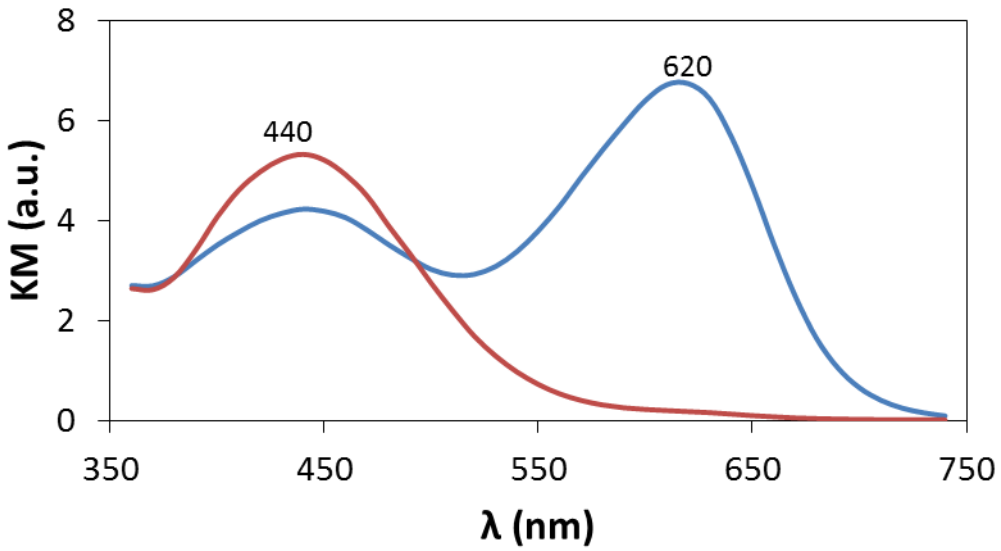

Fig. 4. Kubelka Munk diffuse reflectance spectra of the TB pigment powder (as illustrated in Fig. 2) under 0 (blue line) and 100% of CO_2.

3.3. The TB plastic film: gaseous CO_2

The absorbance spectrum of the TB plastic film was studied as a function of the ambient level of gaseous CO_2 (0% to 100%) and the results are illustrated in Fig. 5.

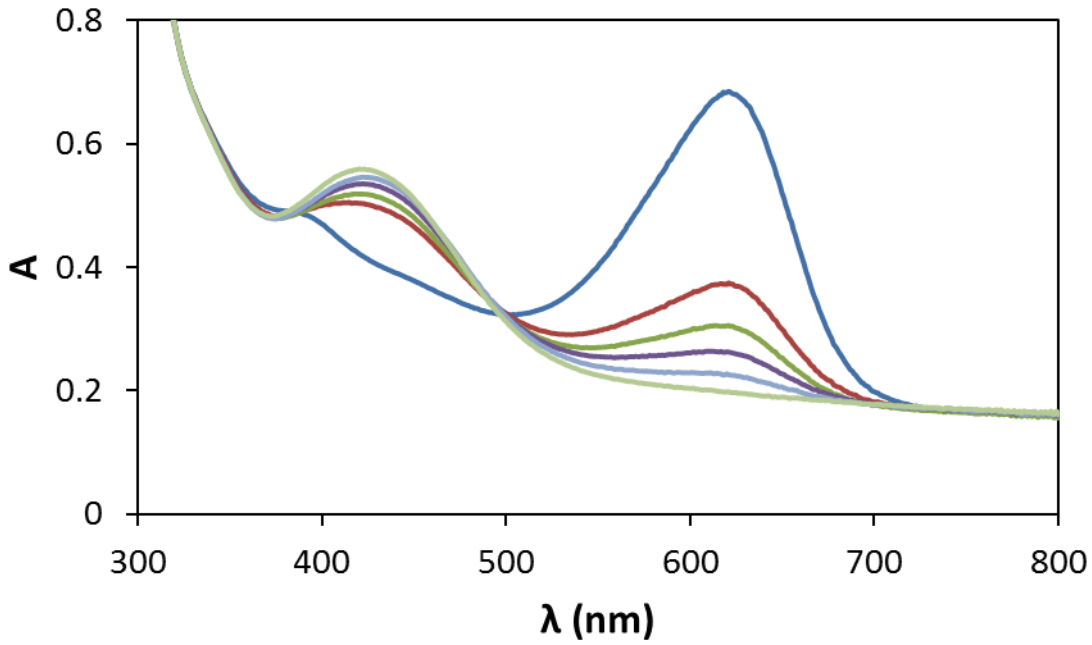

Fig. 5. UV-vis absorbance spectra of thymol blue plastic film recorded when exposed to different %CO_2/Ar gas phase compositions. The %CO_2 levels used were (from top to bottom): 0, 0.1, 0.3, 0.4, 1 and 100%.

From the data in Fig. 5 it is clear the absorbance exhibited by the deprotonated form of the TB plastic film, D^-, (λ_{max} = 621 nm) decreases with increasing %CO_2 in the ambient gas stream, as TB^- is converted to HTB, via reaction (1). A plot of the absorbance at λ_{max} = 621 nm, as a function of %CO_2, gleaned from the spectra illustrated in Fig. 5, is illustrated in Fig. 6, along with a plot of *R* vs %CO_2 as the insert diagram, where *R* was calculated using eqn(2) and the absorbance data in the main diagram. The latter plot reveals a value for %CO_2(S=1/2) = 0.063%, which suggests that the TB plastic film is extremely sensitive to the ambient level of gaseous CO_2 and more sensitive than many other reported similar PT-based CO_2 sensors (see table 1). The limit of detection, LOD, was calculated as 0.006% CO_2.

When the CO_2-containing purge gases used above were saturated with water vapour, i.e. 100% RH, and passed over a TB plastic film, the λ_{max} for the TB^-, in the TB plastic film, underwent a hypsochromatic shift from 621 nm to 613 nm, and the film appeared ca. 3x's less sensitive towards CO_2, i.e. %CO_2(S=1/2) = of 0.20%, with an LOD of 0.01%.

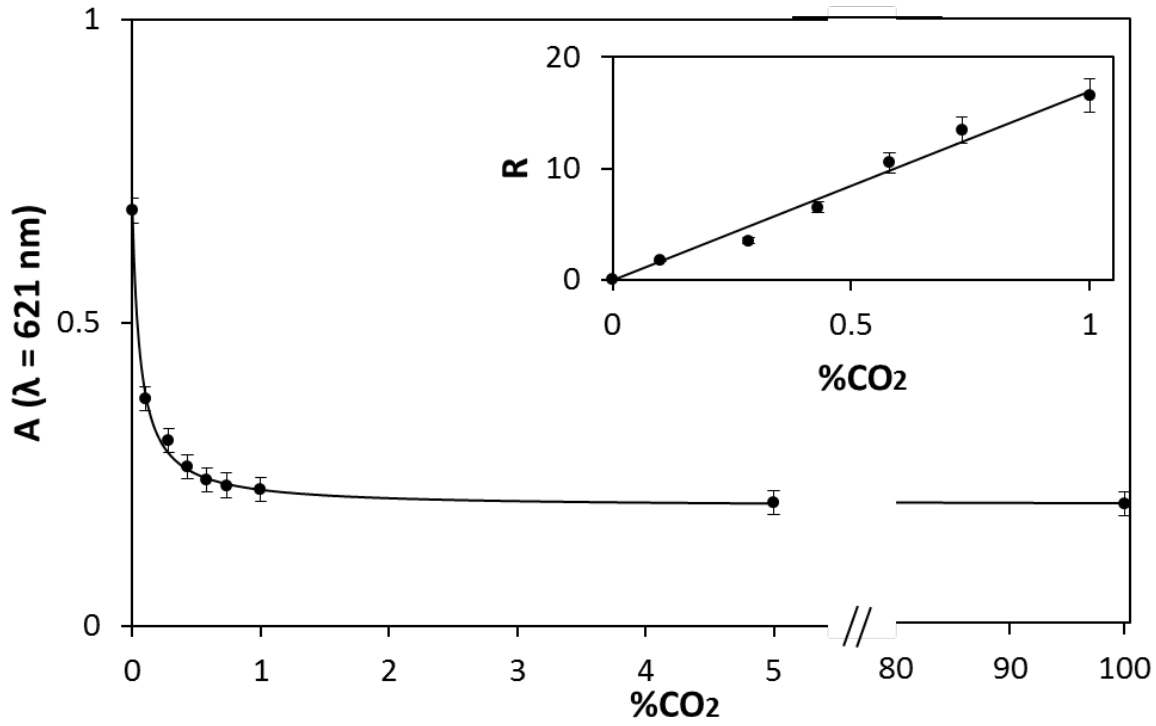

Fig. 6. Plot of absorbance of a TB film at 621 nm versus $\%CO_2$ in the dry gas stream. The insert plot of the data in the main diagram, in the form of *R*, see eqn (2), vs $\%CO_2$ reveals a good straight line with a gradient (= α) = 15.9%$^{-1}$ and thus a $\%CO_2$(S=1/2) value of 0.063%.

Although the exact cause for the marked decrease in the CO_2 sensitivity of the TB plastic film in humid air (and – it turns out – in HS water too, *vide infra)* is not clear, it is likely to be associated with a change in the microenvironment surrounding the LDPE encapsulated TB-ink coated silica pigment particles due, in turn, to an increased water content of the film. Evidence for this is provided by: (i) the observation of a slightly increased haziness in the film (Δabsorbance (λ = 513 nm) = 0.09) and (ii) the shift in the absorbance λ_{max} for the TB film from its usual value of 621 nm for a dry film, to 613 nm in humid air (and 603 nm in HS water). The latter is particular interesting as the absorbance λ_{max} for TB^- dissolved in water is ca. 596 nm. This finding suggests that, notwithstanding the presence of the highly hydrophobic LDPE, the TB pigment particles take up sufficient water vapour from the ambient humid gas phase to render their microenvironment almost water like. The effects produced by an increase in polarity of the microenvironment, signified by the negative shift in the value for λ_{max} for a dry TB plastic film, brought about by the presence of a high (100%) RH or immersion of the TB film into HS water, are likely to include: (i) a decrease in the pK_a of TB and (ii) a decrease in the solubility of CO_2 (for example the solubility of CO_2 is 17 times

higher in trichloromethane than it is in water) [38]. Both of these effects are likely to produce a measurable decrease in the CO_2 sensitivity exhibited by the TB film when highly hydrated, as opposed to dry. It is also worth noting that this overall loss of sensitivity, brought about by a high ambient RH or immersion of the film in HS water, is readily reversed by returning the TB plastic film to a dry atmosphere.

The ability of the TB plastic film to respond to a sudden and striking change in $\%CO_2$ was investigated using an alternating stream of 0% (i.e. Ar) and 1% CO_2. The results of this work revealed that, in the gas phase, the sensor exhibits a 90% response time ($t_{50\downarrow}$) of ca. 3 min, and a 50% recovery time ($t_{50\uparrow}$) of ca. 32 min. Thus, compared to the TB pigment, and most conventional, ink-based, CO_2 optical sensors (typical $t_{50\downarrow}$ & $t_{50\uparrow}$ times of: 4 and 7 s) [33], the TB plastic film has relatively long response and recovery times in making gas phase CO_2 measurements . However, this is not too surprising given that the TB plastic film is much thicker, i.e. ca. 47.5 $\pm$ 2.5 μm, than that of most ink-based CO_2 sensors (1-8 microns). The response and recovery times of most CO_2 optical sensors depend directly upon the rate of diffusion of the CO_2 into and out of the sensor film, with a proportionality constant that is inversely proportional to the square of the film thickness [39]. Thus, by using a narrower film die to extrude the film it should be possible to create sufficiently thin TB plastic film (say 15 μm) to compete with the low $t_{50\downarrow}$ & $t_{50\uparrow}$ times exhibited by most CO_2 sensor ink films [33].

For comparison purposes, a classic solvent-based, naked PT TB ink film sensor for CO_2 was made according to a previously-reported recipe [26] and its sensitivity towards CO_2 was then assessed as described above for the TB plastic film. The TB ink film (comprising TB in ethyl cellulose, with TBAH as the base and tributylphosphate as the plasticiser) exhibited a similar sensitivity and LOD towards **gaseous** CO_2, i.e. $\%CO_2(S=1/2)$ = 0.08% and 0.001%, respectively, as that of the TB plastic film, i.e. $\%CO_2(S=1/2)$ = 0.06% and 0.01%. Note that here, and elsewhere [26], work shows that the TB ink film has a very limited stability when used to detect dissolved CO_2 and fails within minutes, when placed in aqueous solution with a pH < 6 or an ionic strength > 0.01 M. As a result it is entirely inappropriate for making any dissolved CO_2 measurements and, its response is consistent with the fact that many of the

CO_2 sensor ink films listed in table 1 require an additional GPM layer in order to allow them to monitor dissolved CO_2.

3.4. The TB plastic film: dissolved CO_2 sensor

In this work a pre-soaked TB plastic film was placed in a cuvette containing HS water. Different, known levels of CO_2, spanning the range 0-100% CO_2, were then bubbled through the HS water for at least 45 min to ensure complete saturation, after which, in each case, the UV/Vis absorption spectrum of the film was recorded.

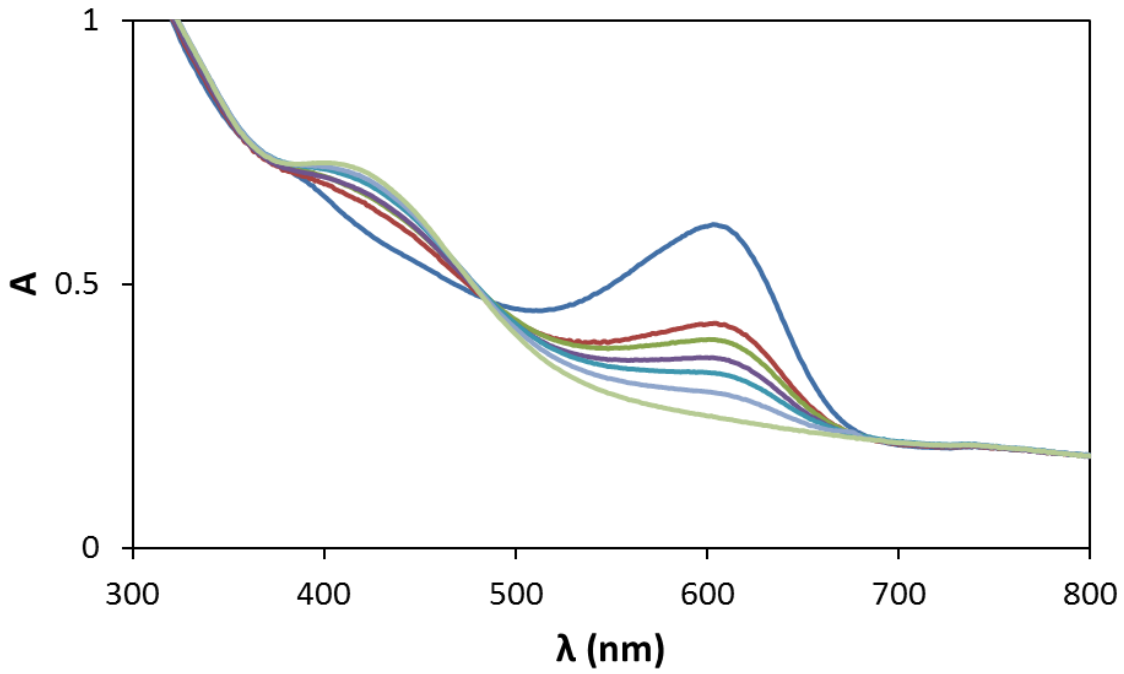

Fig. 7. UV-vis absorbance spectra of a typical TB film in HS water saturated with the following different percentages of CO_2 (from top to bottom): 0, 0.1, 0.3, 0.4, 0.6, 1 and 100%.

The results of this work are illustrated in Fig. 7 and reveal that, as expected, the absorbance of the TB film due to TB^-, with a λ_{max} value = 603 nm, decreases with increasing $\%CO_2$. A plot of the absorbance at 603 nm vs $\%CO_2$ data, along with an the insert plot of *R* vs $\%CO_2$, are illustrated in Fig. 8 and the latter reveals a good straight line, in accordance with eqn (2), with a gradient (α) = 5.6 $\%^{-1}$, i.e. a $\%CO_2$(S=1/2) value of 0.18%, which is very similar to that exhibited by the TB plastic film when in a humid (100% RH) gas phase. The LOD for CO_2 for

the TB film in HS water was the same as that in humid gas, i.e. 0.01%, showing that the TB film is as sensitive towards CO_2 in HS water as it is in humid gas.

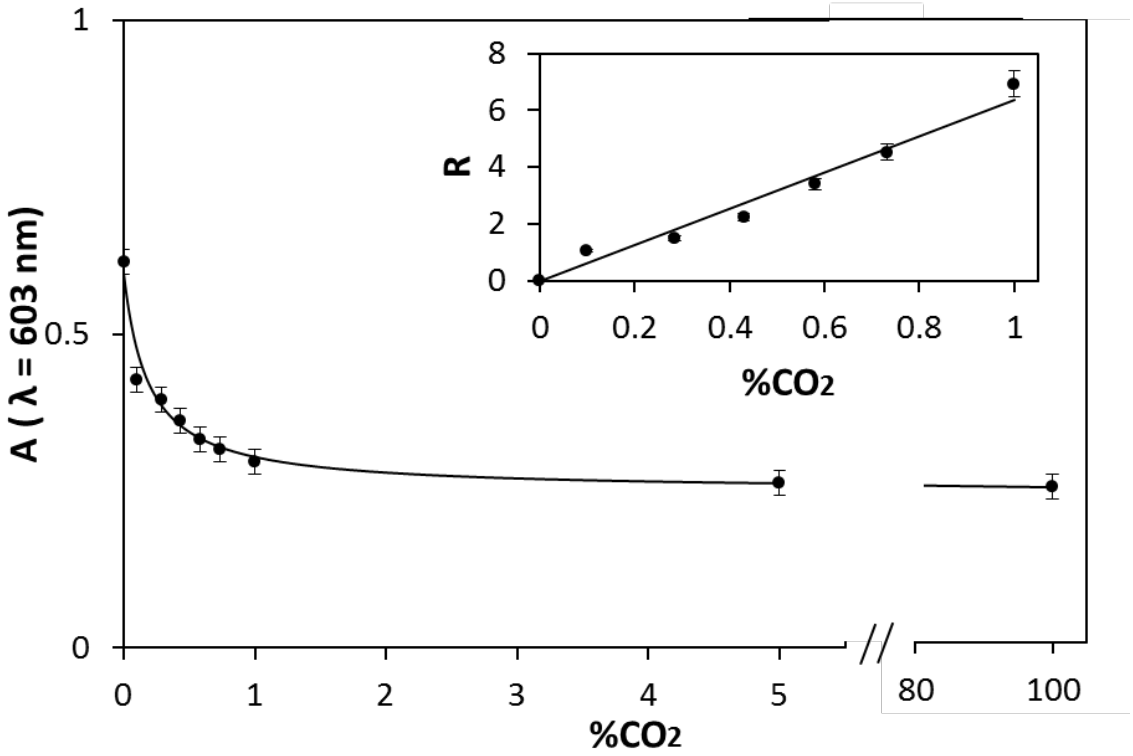

Fig. 8. Plots of absorbance of TB plastic film in HS water at 603 nm versus %CO_2. Insert plot of *R*, derived from the absorbance date in the main plot and eqn (2), vs % CO_2 yields a line of best fit with a gradient = α = 5.6 $\%^{-1}$.

The following sections describe the results of further probing of the characteristics of the TB plastic film in monitoring dissolved CO_2 levels in HS water.

3.5. Effect of temperature

Reaction (1), the underlying process behind all PT-based CO_2 optical sensors, including the TB plastic film reported here, is spontaneous and involves a decrease in system entropy, as the gaseous CO_2 reacts with the $Q^+D^-.xH_2O$ ion-pair, to form a bicarbonate salt. From basic thermodynamics, it follows that the equilibrium constant for reaction (1), a measure of which is the value of α, will decrease with increasing temperature, as predicted by the van't Hoff reaction isochore. Thus, all PT-based CO_2 optical sensors are temperature sensitive, and decrease in CO_2 sensitivity with increasing temperature [24,25]. The TB plastic film

reported here is no exception, as revealed by the results of a series of calibration curves (i.e. absorbance vs %CO_2 curves) recorded at different temperatures, spanning the range 0-31°C in HS water. The latter data were used to generate the appropriate *R* vs %CO_2 plots for the different temperatures studied, illustrated in Fig. 9, from which values of the gradient for the different temperatures, i.e. α(T), were determined. An Arrhenius plot of this data, i.e. ln(α(T)) vs 1/T, revealed an activation energy for reaction (1) for the TB plastic film CO_2 sensor of 21.1 ± 4.2 kJ mol^{-1} which is similar to that of 26.8 ± 1.0 kJ mol^{-1} reported [40] by others for a TB-$Ru(bpy)_3^{2+}$ based FRET CO_2 sensor (polymer: ethyl cellulose; phase-transfer agent: TOAH).

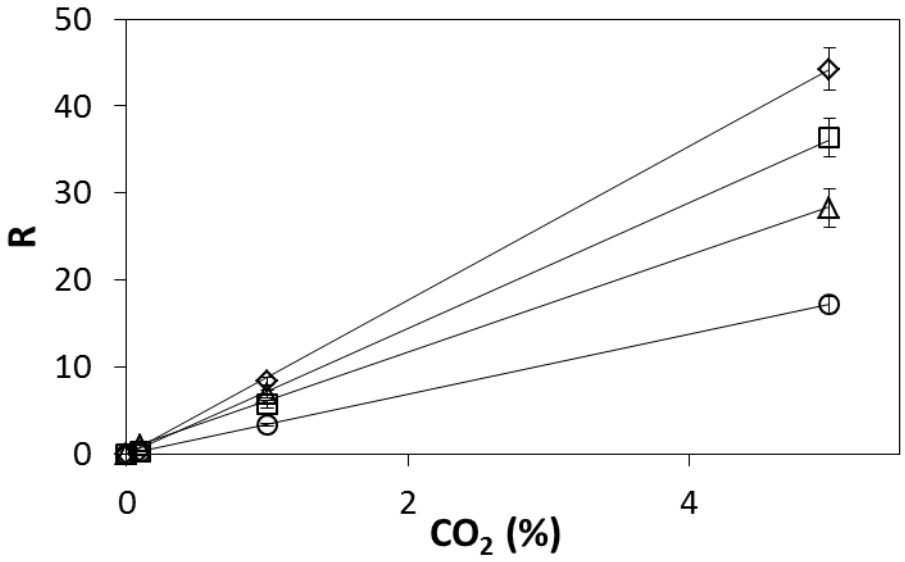

Fig. 9. R vs %CO_2 plots of thymol blue plastic film in HS water under different temperature, from top to bottom: 0.6, 11.3, 21.8, 30.7**°**C.

3.6. Storage in air

One of the most striking features of the TB plastic film is its stability in air. For example, when stored under ambient atmospheric conditions, in the dark, the film is stable for > 8 months, showing no loss in sensitivity. In contrast, and as illustrated by the photographs in the supplementary information, Fig. S1, a typical TB solvent-based CO_2 sensitive ink film lasts only ca. 4-5 days under the same conditions, before losing its blue/green colour and changing to its yellow protonated form. As noted earlier, the lack of stability exhibited by many PT-based CO_2 ink film sensors is usually attributed to a loss of water (if kept in a dry

atmosphere) and possible permanent reaction with common, albeit low level, acidic pollutants, such as SO_2 and NO_2 [31]. Others have noted that the stability of the latter films can be improved markedly by storing them either in water [30], in a very humid (usually RH ≥ ca. 80%) atmosphere [41], or with sodium carbonate (as a sink for volatile acidic volatiles) in the dark [40]. Obviously, the need for such storage conditions then places a constraint on the commercial potential of such CO_2 ink film sensors, whereas, in contrast, the TB plastic film sensor reported here appears very stable when stored under ambient, dark conditions. However, these films, as with most dye-containing sensor films, will photobleach with time if left exposed to sunlight for long periods of time, thus the need for dark storage conditions.

3.7. Drift in HS water

In order to probe the stability, and functionality, of the TB film in HS water further, a typical TB film was placed in a 1 cm cuvette filled with HS water and stored in 0.1% saturated CO_2 water for over 7 days. The HS water was flushed once every day with 1% CO_2, before being returned to a background 0.1% CO_2 saturation level and the absorbance of the TB plastic film, at 600 nm, monitored throughout. The results of this work are illustrated in Fig. 10 and show that in HS water the film's sensitivity (towards CO_2) remains high and shows little evidence of dye leaching over a 7 day period, with a drift in initial absorbance of < 0.3% per day.

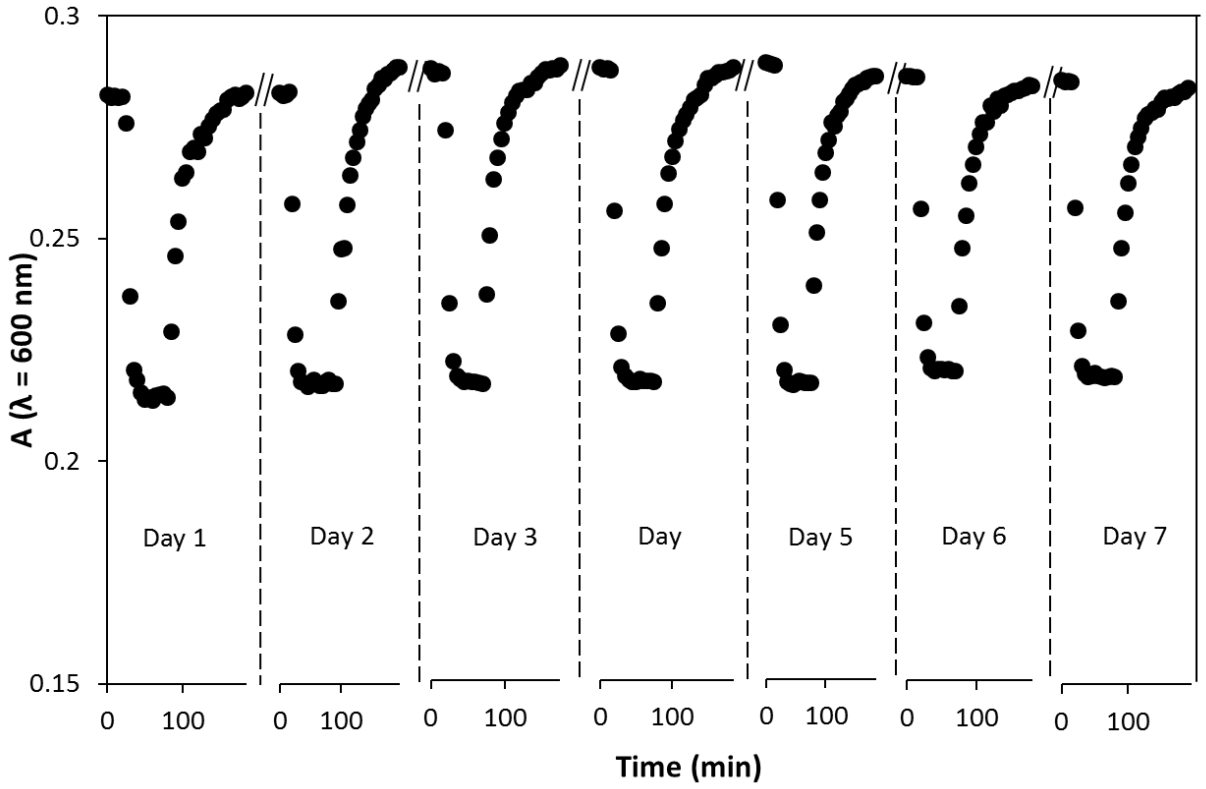

Fig. 10. Plots of absorbance of thymol blue plastic film in HS water alternatively purged through 0.1%CO_2 and 1%CO_2, and repeated for 7 days.

From this work the calculated 50% response $t_{50\downarrow}$ (0.1% to 1% CO_2) and 50% recovery (1% to 0.1% CO_2) $t_{50\%\uparrow}$ times for the TB plastic film, when used for dissolved CO_2 measurements, were 5 min and 15 min, respectively. These response and recovery times are obviously completely inadequate for the monitoring of rapid changes in dissolved CO_2, as required for blood gas monitoring for example, where the %CO_2 is typically 5%. A Severinghaus electrode for example is often able to respond in a minute, although this can be considerably longer if it possesses a large volume internal bulk electrolyte, or if the concentrations of CO_2 are low [22,42,43]. For example, Xi and Bakker [22] report that, for a shift in CO_2 saturation from 0.04% to 0.66%, the Severinghaus probe takes at least 5 min to stabilise to its new potential. Interestingly, this is the probe's 'response time', as the concentration of CO_2 has been increased, and it follows, from the work of others [42,43], that the associated recovery time for the probe will be longer, possibly by a factor of 4, which implies a recovery time of ca. 20 min. Note that the CO_2 saturation values used by Xi and Bakker [22] (0.04% to 0.66%) in their work on a Severinghaus electrode are not too dissimilar to those used here for the

TB film (0.1% to 1%) in Fig. 11, which suggests that the 47.5 µm, TB plastic film has a similar response time, and probable recovery time, very similar to that of the Severinghaus electrode used by Xi and Bakker [22], when responding to these very low levels of CO_2. However, in order to demonstrate that the TB plastic film can be made to respond much faster simply by making it thinner, a 15 µm, as opposed to the usual 47.5 µm, TB plastic film was prepared and subjected to the same alternative purging in HS water as described in Fig. 10. This short study showed that the thin film exhibits the same sensitivity, i.e. same value for α, but much shorter with $t_{50\downarrow}$ (0.1% to 1% CO_2) and $t_{50\%\uparrow}$ (1% to 0.1% CO_2) times of 2 min and 6 min, than the thick film sensor. The latter response and recovery times appear reasonable, if only for use in long-term monitoring of CO_2 levels in aquatic systems, but open for further improvement.

3.8. Stability in acidic solution

Another striking advantage of the TB plastic film CO_2 sensor over most other naked optical CO_2 sensors, is its marked high-stability when used in very acidic (pH ≤ 2) solution. As noted earlier, most 'naked' optical CO_2 sensors, including the commercial PreSens GmbH, fluorescent-based, dissolved CO_2 sensor, cannot be used for any significant period of time at pH's < 4 [32]. In contrast, the TB plastic film sensor reported here shows no loss of function, or dye, when stored in 0.01 M HCl aqueous solution for at least for 3 hours. Evidence of the ability of the TB plastic film to function as a CO_2 sensor in aqueous solution, regardless of pH, is provided by the series of photographic images illustrated in the supplementary information, Figs. S2 and S3. From this work, it is clear that upon dipping the TB film into sparkling, i.e. carbonated, water, the TB^-, in the TB plastic film is readily protonated (green/blue to yellow), within 1 min, and its original colour is restored upon its removal from the sparkling water. As illustrated by the pictures in Fig. S3 show that when the same TB plastic film is placed in a 0.01 M HCl aqueous solution the film's green colour remains unaltered, but changes to yellow, via reaction (1), upon bubbling CO_2 through the solution. When the yellow TB film is withdrawn from the aqueous acidic solution, it regains its original green colour within minutes.

Other work showed that the TB plastic film was unresponsive to pH when placed, for at least 1 h, in HS water with its pH adjusted to either: 8.4, 6.4, 4.3 or 2.3, thereby providing additional evidence that the TB plastic film responds to dissolved CO_2 and not pH.

From the results of this work, it appears that the LDPE acts both as a sensor pigment encapsulation medium and an intrinsic GPM, protecting the sensor TB pigment particles from dye leaching and acid attack. As a consequence, the TB plastic film sensor is easier and less expensive to construct than most reported optical sensors for dissolved CO_2 detection.

4. Conclusions

Table 2 below provides a summary of the main results reported here for all the CO_2 sensors/environments tested, i.e. (a) the TB plastic film in: (i) a dry and wet (RH = 100%) gas phase and (ii) HS water and (b) a TB ink film in a dry gas phase, reported above. These results include: the measured absorbance λ_{max} values (due to TB^-), CO_2 sensitivity values (i.e. α and $\%CO_2(S=1/2)$ values), and associated limits of detection (LOD) values for all the CO_2 sensors/environments. An inspection of these results shows that the TB plastic film is ca. 3x's more sensitive when used to detect the 100% dry gaseous CO_2 than dissolved or humid CO_2. In addition, it can be seen that the TB plastic film is similar in sensitivity to that of a conventional TB ink film, when used to detect gaseous CO_2. The results in HS water are particularly remarkable given that the TB plastic film has no additional GPM, and yet is an effective, stable and highly sensitive sensor for CO_2 in this highly saline medium. In addition, it appears able to tolerate high levels of acidity and has a long storage lifetime when kept in the dark, but otherwise ambient conditions, in contrast with most other PT-based optical sensors for CO_2 (see table 1). Like many CO_2 optical sensors, the TB plastic film's CO_2 sensitivity decreases with increasing temperature ($\Delta H = 21.1 \pm 4.2$ kJ mol^{-1}).

Table 2: Absorbance and response characteristics of the TB based CO_2 sensors reported in this work

TB Sensor	λ_{max} (nm)	R	α ($\%^{-1}$)	$\%CO_2$ (S=1/2)	LOD %
TB plastic film in dry gas	621	79.8	15 ± 2	0.06	0.006
TB plastic film in 100% humid gas	613	22.0	4.4 ± 0.1	0.20	0.01
TB plastic film in HS water	603	23.0	5.6 ± 0.1	0.18	0.01
TB solvent-based ink film in dry gas	626	62.8	12.5 ± 0.3	0.08	0.005

The CO_2 sensitivity of the current TB film ($\%CO_2$(S=1/2) = 0.18% ≡ 1800 μatm) is a little too high for monitoring the usual level of dissolved CO_2 found in sea water (ca. 0.035%). However, there are many instances in the hydrosphere where relevant higher levels are found including: eutrophic lakes (87% of Florida lakes have supersaturated levels of CO_2) [44,45], ocean depths (at which significant CO_2 sequestration occurs) [46] and fish farms [47,48]. By choosing a different pH-sensor dye with a higher pK_a, a more sensitive CO_2 sensor could be constructed and *vice versa* [37]. And, by making the film much thinner, the indicator may find application in areas where the rapid monitoring of CO_2 is required, such as in the rapid analysis of clinical blood samples or the rapid depth profiling of aquatic systems.

Acknowledgements

We thank the DAFM for funding this work (FIRM project ref: 11/F/015)

References

[1] J. N. Butler, Carbon dioxide equilibria and their applications, CRC Press, Boca Raton, FL. 1991.

[2] E. Rabinowitch, Govindjee, Photosynthesis, John Wiley & Sons, New York 1969.

[3] C.L. Lake, Clinical Monitoring, W.B. Saunders Co., Philadelphia 1990.

[4] C. Moore, A. Barnard, P. Fietzek, M.R. Lewis, H.M. Sosik, S. White, O. Zielinski, Optical tools for ocean monitoring and research, Ocean Sci. 5 (2009) 661-684.

[5] O.S. Wolfbeis, Fiber-optic sensors in bioprocess control. In: Twork, J.V., Yacynych, A.M. (Eds.), Sensors in Bioprocess Control. Marcel Dekker, New York 1990.

[6] J. Zosel, W. Oelßner, M. Decker, G. Gerlach, U. Guth, The measurement of dissolved and gaseous carbon dioxide concentration, Meas. Sci. Technol. 12 (2001) 1-45.

[7] S. Neethirajan, D.S. Jayas, S. Sadistap, Carbon dioxide (CO_2) sensors for the agri-food industry — a review, Food and Bioprocess Technology 2 (2009) 115-121.

[8] J.A. Breland II, R.H. Byrne, Determination of sea water alkalinity by direct equilibration with carbon dioxide, Anal. Chem. 64 (1992) 2306-2309.

[9] D.R. Walt, G. Gabor, Multiple-indicator fiber-optic sensor for high-resolution pCO_2 sea water measurements, Anal. Chim. Acta 274 (1993) 47-52.

[10] M.S. Johnson, M.F. Billett, K.J. Dinsmore, M. Wallin, K.E. Dyson, R.S. Jassal, Direct and continuous measurement of dissolved carbon dioxide in freshwater aquatic systems—method and applications, Ecohydrology 3 (2010), 68-78.

[11] R.F. Weiss, Determinations of Carbon Dioxide and Methane by Dual Catalyst Flame Ionization Chromatography and Nitrous Oxide by Electron Capture Chromatography, J. Chromatography 19 (1981) 611-616.

[12] D. Dyrssen, A gran titration of sea water on board Sagitta, Acta Chem. Scand. 19 (1965) 1265.

[13] K.M. Johnson, A.E. King, J.M. Sieburth, Coulometric TCO2 analyses for marine studies; an introduction, Marine Chemistry 16 (1985) 61-82.

[14] T. Ishiji, D.W. Chipman, T. Takahashi, K. Takahashi, Amperometric sensor for monitoring of dissolved carbon dioxide in seawater, Sensors and Actuators B 76 (2001) 265-269.

[15] J.W. Severinghaus, First electrodes for blood PO2 and PCO2 determination, J. Appld. Physiol. 97 (2004) 1599-1600.

[16] P. Bühlmann, E. Pretsch, E. Bakker, Carrier-based ion-selective electrodes and bulk optodes. 2. Ionophores for potentiometric and optical sensors, Chem. Rev. 98 (1998) 1593-1687.

[17] Z.A. Wang, X. Liu, R.H. Byrne, R. Wanninkhof, R.E. Bernstein, E.A. Kaltenbacher, J. Patten, Simultaneous spectrophotometric flow-through measurements of pH, carbon dioxide fugacity, and total inorganic carbon in seawater, Anal. Chim. Acta 596 (2007) 23-36.

[18] M.B. Tabacco, M. Uttamlal, M. McAllister, D.R. Walt, An autonomous sensor and telemetry system for low-level pCO2 measurements in seawater, Anal. Chem. 71 (1999) 154-161.

[19] A.I Abdullah, E. Eek, Automatic method for the determination of total CO2 in natural waters, Wat. Res. 29 (1995) 1231-1234.

[20] X. Xie, M. Pawlak, M.L. Tercier-Waeber, E. Bakker, Direct optical carbon dioxide sensing based on a polymeric film doped with a selective molecular tweezer-type ionophore, Anal. Chem. 84 (2012) 3163-3169.

[21] Y.S. Choi, L.L. Lvova, J.H. Shin, S.H. Oh, C.S. Lee, B.H. Kim, G.S. Cha, H. Nam, Determination of oceanic carbon dioxide using a carbonate-selective electrode, Anal. Chem. 74 (2002) 2435-2440.

[22] X. Xi, E. Bakker, Non-Severinghaus potentiometric dissolved CO2 sensor with improved characteristics, Anal. Chem. 85 (2013) 1332-1336.

[23] P. Puligundla, J. Jung, S. Ko, Carbon dioxide sensors for intelligent food packaging applications, Food Control 25 (2012) 328-333.

[24] A. Mills, Q. Chang, N. McMurray, Equilibrium studies on colorimetric plastic film sensors for carbon dioxide, Anal. Chem. 64 (1992) 1383-1389.

[25] A. Mills, K. Eaton, Optical Sensors for Carbon Dioxide: An Overview of Design and Sensing Strategies Past and Present, Quim. Anal. 19 (2000) 75-86.

[26] A. Mills and Q. Chang, Colourimetric Polymer Film Sensors for Dissolved Carbon Dioxide, Sensors and Actuators B 21 (1994) 83-89.

[27] N. Lefèvre, J.P. Ciabrini, G. Michard, B. Brient, M. DuChaffaut, L. Merlivat, A new optical sensor for PCO2 measurements in seawater, Marine Chemistry 42 (1993) 189-198.

[28] O. Oter, K. Ertekin, D. Topkaya, S. Alp, Room temperature ionic liquids as optical sensor matrix materials for gaseous and dissolved CO2, Sensors and Actuators B 117 (2006) 295-301.

[29] G. Neurauter, I. Klimant, O.S. Wolfbeis, Fiber-optic microsensor for high resolution pCO2 sensing in marine environment, Fresenius J. Anal. Chem. 366 (2000) 481–487.

[30] O.S. Wolfbeis, B. Kovács, K. Goswami, S.M. Klainer, Fiber-Optic Fluorescence Carbon Dioxide Sensor for Environmental Monitoring, Mikrochim. Acta 129 (1998) 181-188.

[31] S.M. Borisov, C. Krause, S. Arain, O.S. Wolfbeis, Composite material for simultaneous and contactless luminescent sensing and imaging of oxygen and carbon dioxide, Adv. Mater. 18 (2006) 1511–1516.

[32] Presens CO2-sensors. http://www.presens.de/products/brochures/category/sensor-probes/brochure/co2-sensors.html#tab-intro (accessed March 2016).

[33] A. Mills, D. Yusufu, Highly CO2 sensitive extruded fluorescent plastic indicator film based on HPTS, Analyst 141 (2016) 999-1008.

[34] A. Mills, N. Wells, Indoor and outdoor monitoring of photocatalytic activity using a mobile phone app. and a photocatalytic activity indicator ink (paii), J. Photochem. Photobiol. A 298 (2015) 64-67.

[35] A. Mills, Optical sensors for carbon dioxide and their applications in: M. -I. Baraton (Eds) Sensors for Environment, Health and Security, Springer, UK 2009.

[36] A. Mills, G.A. Skinner, Water-based colourimetric optical indicators for the detection of carbon dioxide, Analyst 135 (2010) 1912-1917.

[37] A. Mills, Q. Chang, Tuning colourimetric and fluorimetric gas sensors of carbon dioxide, Anal. Chim. Acta 285 (1994) 113-123.

[38] W. Kunerth, Solubility of CO2 and N2O in certain solvents, Phys. Rev. 19 (1921) 512–524.

[39] A. Mills, Q. Chang, Modelled Diffusion-controlled Response and Recovery Behaviour of a Naked Optical Film Sensor with a Hyperbolic-type Response to Analyte Concentration, Analyst 117 (1992) 1461-1466.

[40] G. Neurauter, I. Klimant, O.S. Wolfbeis, Microsecond lifetime-based optical carbon dioxide sensor using luminescence resonance energy transfer, Anal. Chem. Acta 82 (1999) 67-75.

[41] J. Sipior, S. Bambot, M. Romauld, G.M. Carter, J.R. Lakowicz, G. Rao, A life-time based optical CO2 gas sensor with blue or red excitation and stokes or anti-stokes detection, Anal. Biochem. 227 (1995) 309-318.

[42] B. Van Der Schoot, P. Bergveld, Prediction of the dynamic response of the potentiometric carbon dioxide electrode, Anal. Chim. Acta. 166 (1984) 93-101.

[43] T. Samukawa, K. Ohta, M. Onitsuka, M. Ito, R. Motohashi, Numerical approach to the explanation of the response time of the Severinghaus type electrode, Anal. Chim. Acta, 316 (1995) 83-92.

[44] M.B. Balmer, J.A. Downing, Carbon dioxide concentrations in eutrophic lakes: undersaturation implies atmospheric uptake, Inland Waters 1 (2011) 125-132.

[45] J.K. Lazzarino, R.W. Bachmann, M.V. Hoyer, D.E. Canfield Jr, Carbon dioxide supersaturation in Florida lakes, Hydrobiologia 627 (2009) 169–180.

[46] Y. Watanabe, A. Yamaguchi, H. Ishida, T. Harimoto, S. Suzuki, Y. Sekido, T. Ikeda, Y. Shirayama, M.M. Takahashi, T. Ohsumi, J. Ishizaka, Lethality of Increasing CO2 Levels on Deep-Sea Copepods in the Western North Pacific, Journal of Oceanography 62 (2006) 185-196.

[47] A. William, M.D. Robert, Interactions of pH, Carbon Dioxide, Alkalinity and Hardness in Fish Ponds, SRAC publication, 1992 December, No. 464. http://www2.ca.uky.edu/wkrec/InteractionspHEtc.PDF (accessed March, 2016).

[48] Y. Ulgenes, A. Seland, T. Lunde, Modeling water quality for seawater aquaculture in: H. Reinersten, L. A. Dahle, L. Jorgensen (Eds) Fish farming technology, CRC Press, Norway 1993.